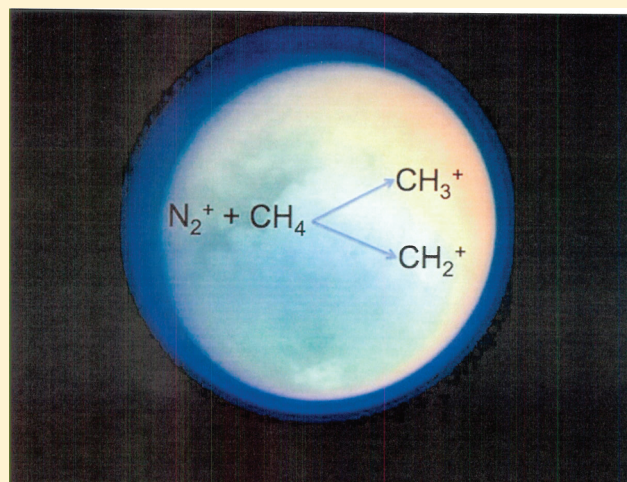


# Primary Branching Ratios for the Low-Temperature Reaction of State-Prepared $\text{N}_2^+$ with $\text{CH}_4$ , $\text{C}_2\text{H}_2$ , and $\text{C}_2\text{H}_4$

Wilson K. Gichuhi and Arthur G. Suits\*

Department of Chemistry, Wayne State University, Detroit Michigan 48202, United States

**ABSTRACT:** Product branching ratios (BRs) are reported for ion–molecule reactions of state-prepared nitrogen cation ( $\text{N}_2^+$ ) with methane ( $\text{CH}_4$ ), acetylene ( $\text{C}_2\text{H}_2$ ), and ethylene ( $\text{C}_2\text{H}_4$ ) at low temperature using a modified ion imaging apparatus. These reactions are performed in a supersonic nozzle expansion characterized by a rotational temperature of  $40 \pm 5\text{ K}$ . For the  $\text{N}_2^+ + \text{CH}_4$  reaction, a BR of 0.83:0.17 is obtained for the dissociative charge-transfer (CT) reaction that gives rise to the formation of  $\text{CH}_3^+$  and  $\text{CH}_2^+$  product ions, respectively. The  $\text{N}_2^+ + \text{C}_2\text{H}_2$  ion–molecule reaction proceeds through a nondissociative CT process that results in the sole formation of  $\text{C}_2\text{H}_2^+$  product ions. The reaction of  $\text{N}_2^+$  with  $\text{C}_2\text{H}_4$  leads to the formation of  $\text{C}_2\text{H}_3^+$  and  $\text{C}_2\text{H}_2^+$  product ions with a BR of 0.74:0.26, respectively. The reported BR for the  $\text{N}_2^+ + \text{C}_2\text{H}_4$  reaction is supportive of a nonresonant dissociative CT mechanism similar to the one that accompanies the  $\text{N}_2^+ + \text{CH}_4$  reaction. No dependence of the branching ratios on  $\text{N}_2^+$  rotational level was observed. In addition to providing direct insight into the dynamics of the state-prepared  $\text{N}_2^+$  ion–molecule reactions with the target neutral hydrocarbon molecules, the reported low-temperature BRs are also important for accurate modeling of the nitrogen-dominated upper atmosphere of Saturn’s moon, Titan.



## INTRODUCTION

The gas-phase study of state-specific ion–molecule reactions<sup>1</sup> has provided an essential cornerstone for the fundamental understanding of unimolecular and bimolecular reaction dynamics.<sup>23</sup> State-specific ion–molecule reaction experiments<sup>4,5</sup> have, in addition, been very useful in developing accurate models of plasma environments and planetary atmospheres through the determination of absolute state-selected cross sections<sup>6,7</sup> and product BRs.<sup>8,9</sup> The application of powerful methods that probe ion–molecule reactions under single collision conditions<sup>10,11</sup> and reaction kinetics at the relevant temperatures are key to developing a comprehensive picture of ion–molecule reaction dynamics.<sup>12,13</sup> A great challenge facing these approaches, however, is obtaining accurate branching ratios at the low temperatures characteristic of the atmospheres of the outer planets and their satellites. Although important contributions to the study of ion–molecule reaction dynamics have been achieved by the use of state-prepared ions as the precursor reactant species in ion–molecule reactions,<sup>5</sup> accurate determinations of BRs of the various product channels have remained a challenging subject of considerable interest because of their critical role in the accurate modeling of chemically active and reducing planetary atmospheres such as the dense nitrogen-rich atmosphere of Titan.

In Titan’s ionosphere, the reaction between  $\text{N}_2^+$  and  $\text{CH}_4$  represents the primary step through which  $\text{N}_2^+$  ions are efficiently destroyed and other reactive radicals such as  $\text{CH}_3^+$  and

$\text{CH}_2^+$  are created.<sup>14,15</sup> The highly reactive radicals and ionic species produced in these ion–molecule collisions further react to generate a plethora of hydrocarbons and nitrogen-bearing species that contribute to the formation of the poorly understood haze in Titan’s atmosphere. Ion–molecule studies related to Titan’s upper atmosphere have long been undertaken because of their potential role in the formation of polyaromatic hydrocarbons (PAHs), nitriles, and other complex molecules<sup>15,16</sup> that constitute the haze layers in Titan’s upper atmosphere. As more concrete and detailed chemical information, such as from Cassini’s ion and neutral mass spectrometer (INMS),<sup>17,18</sup> has emerged, efforts to provide accurate models of Titan’s upper atmosphere have in parallel necessitated the need for accurate and up-to-date laboratory measurements of BRs of the crucial ion–molecule reactions that are important in the ionosphere.<sup>19,20</sup> A substantial number of laboratory studies have been devoted to the accurate determination of BRs of  $\text{N}_2^+$  reactions with the minor hydrocarbon constituents of the upper atmosphere, such as  $\text{CH}_4$ ,  $\text{C}_2\text{H}_2$ , and  $\text{C}_2\text{H}_4$ .<sup>8</sup> As noted by Carrasco et al.,<sup>21,22</sup> the uncertainty in BR

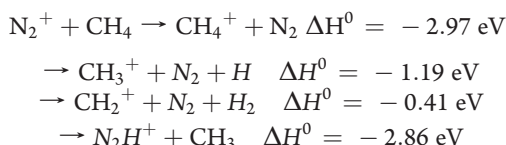
**Special Issue:** A. J. Peter Toennies Festschrift

**Received:** December 31, 2010

**Revised:** March 8, 2011

measurements contributes significantly to a corresponding uncertainty on ion densities predicted by the models. New experimental data are clearly required to provide accurate quantitative comparison between the in situ observations of the Cassini orbiter and the proposed models. Indeed, for a thorough understanding of the astrochemical dynamics<sup>23</sup> in Titan's chemically active atmosphere, new approaches to laboratory measurements of important astrophysical quantities such as the BRs under well-defined conditions need to be developed. To this end, we report on the low-temperature BR measurements of ion–molecule reactions of state-prepared  $N_2^+$  ions with  $CH_4$ ,  $C_2H_2$ , and  $C_2H_4$ . In these studies, we have developed a simple but powerful approach that quickly provides the subject BRs under conditions close to those relevant for Titan's ionosphere.

The possible exoergic reaction pathways for the reactions of  $N_2^+$  with  $CH_4$  are



The  $N_2H^+$  ion product channel has been observed only in the studies of McEwan et al.<sup>20</sup> and Nicolas et al.<sup>6</sup> The channels leading to the formation of  $CH_3^+$  and  $CH_2^+$  product ions have been previously investigated using ion cyclotron resonance (ICR), selected ion flow tube (SIFT), and free jet flow reactor techniques where both the rate coefficients and the BRs were measured.<sup>9,8</sup> However, the BR measured by Randeniya and Smith<sup>24</sup> at 8–15 K differs by 10% from the room-temperature value.<sup>8</sup> The critical role of  $N_2$  photoionization in Titan's atmosphere and its subsequent contribution to the formation of complex organic molecules have also triggered a series of related photocell EUV experiments by Imanaka and Smith.<sup>14,25</sup> These studies have demonstrated that the photoionization of  $N_2^+$  at 60 nm can lead to the formation of  $CH_3^+$  product ions with a subsequent production of complex organic species. However, the conclusions of Smith and Imanaka studies are somewhat limited as to the description of initial chemical reaction mechanisms and the primary branching where ion–molecule reactions are expected to be the dominant processes that determine the subsequent chemistry. This is due to the fact that in a photocell the generation of neutral complex organic molecules is a result of coupled sets of photodissociation, photoionization, ion–molecule reactions, electron–ion recombination, and neutral-molecule reactions.

Whereas the BR measurements for the  $N_2^+ + CH_4$  reaction have been the subject of considerable scrutiny both at room temperature and under low-temperature conditions, the BR data of the various product channels in the reactions of  $N_2^+$  ions with  $C_2H_2$  and  $C_2H_4$  remain insufficiently investigated. Previous work by Anicich et al.<sup>9,8</sup> has generally reported the thermal rate coefficient and BRs using the SIFT technique. For the  $N_2^+ + C_2H_2$  reaction, the most recent study<sup>8</sup> reported a single non-dissociative charge transfer channel leading to the sole formation of  $C_2H_2^+$  product ions. A product branching ratio<sup>9</sup> of 0.37:0.03:0.60 for the formation of  $C_2H_2^+$ ,  $NCH^+$ , and  $N_2H^+$  product ions reported in Anicich et al.'s previous study<sup>9</sup> was believed to be largely in error because of the presence of impurities and secondary collisions. As for the  $N_2^+ + C_2H_4$  reaction, a model by Anicich et al.<sup>8</sup> predicted that the  $C_2H_3^+$  and  $C_2H_2^+$  product ions are formed with an overall BR of 0.64:0.36, respectively, although there is as-yet no experimental support for this determination. This ratio was obtained without invoking

$HCN^+$  and  $HCNH^+$  ions in the model, although they were observed in Anicich et al.'s experiments.

In the present study, we report the product branching ratios of state-prepared  $N_2^+$  ion–molecule reactions with  $CH_4$ ,  $C_2H_2$ , and  $C_2H_4$  in a free jet expansion where the characteristic rotational temperature is  $45 \pm 5$  K and only a few collisions are present. This work is related to a number of previous studies. Pollard and coworkers<sup>26</sup> used REMPI production of  $H_2^+$  to study  $H_2^+ + H_2$ , albeit in crossed beams at superthermal collision energies with an eye to the dynamics. Glenewinkel-Meyer and Gerlich<sup>27</sup> examined the use of REMPI production of state-selected  $H_2^+$  in single beam and merged beam reaction with  $H_2$  and examined many of the underlying experimental issues, but their focus was on using the approach to determine rate constants and cross sections. More recently, Belikov et al.<sup>28</sup> extended the approach described by Glenewinkel-Meyer and Gerlich to study state-specific reactions of  $HBr^+$  at low temperature. They obtained rate constants for several different channels as a function of initial spin–orbit state and rotational level. Our approach is similar, although our focus is simply on determining the branching ratios, and we prepare our reactants in the collision region of the expansion. The BR determinations then provide direct insight into the underlying fundamental mechanisms accompanying the non-resonant dissociative charge-transfer reactions, and these can further assist in the accurate modeling and understanding of the astrochemical dynamics in Titan's ionosphere. Finally, these branching ratio measurements have been undertaken as a test case for our newly commissioned experimental approach that combines state-selective ion preparation with reaction in the course of the nozzle expansion.

## EXPERIMENTAL SECTION

The experiments were carried out using a modified velocity map imaging mass spectrometry apparatus (VMIMS)<sup>29,30</sup> that has been described in detail elsewhere,<sup>31</sup> and hence only details pertinent to the present study are presented here. There are two main modifications from the conventional VMIMS apparatus. One of these is in the source chamber where both the ionization and the reaction of the state-prepared  $N_2^+$  ions with the target neutral molecules take place. For this purpose, we will rename the source chamber and call it the “ionization chamber”. The skimmer has been removed so there is only a large aperture separating this chamber for the chamber housing the ion optics. Another modification is in the velocity-mapping electrodes themselves. The repeller electrode has a 5 mm aperture through which the beam passes, and this is unchanged. However, the larger hole on the extractor electrode is covered with a fine mesh nickel grid to provide homogeneous fields in the ion acceleration region. An application of a negative bias to both the repeller and the extractor plates allows an efficient extraction of the newly born ions into the main chamber for the detection. These are then pulsed to accelerate the ions to the detector and to allow for mass selection. This strategy gives rise to some residual tails in the time-of-flight spectra that likely arise as the spatial spread in the initial ion packet gives rise to an energy spread when the fields are pulsed on. We thus chose to fit the time-of-flight peaks in determining the branching as described below.

The reactant  $N_2^+$  ions were produced via a  $2 + 1$  REMPI scheme.<sup>32</sup> In this scheme, two photons of the 202 nm laser light are used to excite the ground  $N_2$  molecule to the intermediate  $d'' \Sigma_g^+$  Rydberg state. The wavelength calibration of the laser light was achieved by using a wavemeter (coherent wavemaster). The precise frequency of the tripled light used corresponded to the

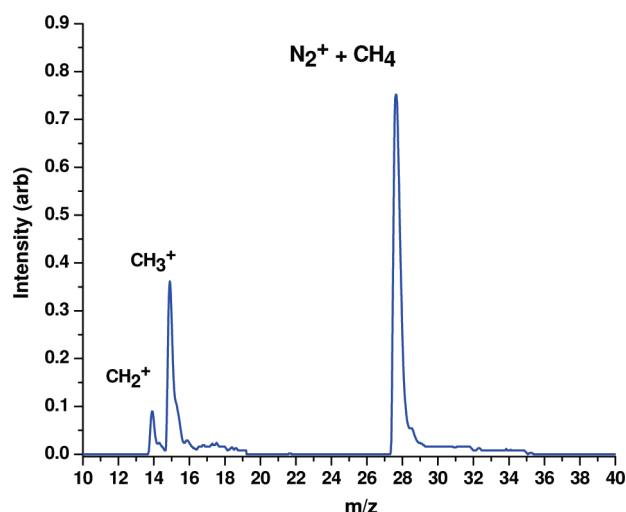


**Figure 1.** Time-of-flight spectrum of the ionic products from the reaction of  $\text{N}_2^+$  ( $\nu = 0$ ) with methane.

transition to the lowest rotational level ( $J = 0$ ) of the  $a'' \Sigma_g^+ \leftarrow X^1\Sigma_g^+$  ( $0, 0$ ) band of  $\text{N}_2$ , measured to be  $49\,420.29 \text{ cm}^{-1}$ . Absorption of an additional photon from the same laser pulse allows the production of  $\text{N}_2^+$  ions. The  $a'' \Sigma_g^+$  Rydberg state possesses a ground-state  $\text{N}_2^+$  core<sup>33,34</sup> and has been shown to ionize exclusively via  $\Delta\nu = 0$ .<sup>35</sup> Consequently, this REMPI produces  $\text{N}_2^+$  ions that are entirely in the ground vibrational state of the cation. We observed no dependence of the branching on the rotational level excited, so these spectra were all obtained on the lowest, most populated level, giving  $\text{N}_2^+$  in low rotational levels. The tunable 202 nm light used to prepare the  $\text{N}_2^+$  ions was generated by frequency tripling of the output of a tunable, narrow-line width ( $<0.075 \text{ cm}^{-1}$ ) OPO laser system (Spectra-Physics MOPO HF). The MOPO HF was pumped by the third harmonic of a seeded Nd/YAG laser operating at 10 Hz. Approximately 50 mJ/pulse of horizontally polarized 607 nm light with 10 ns pulse width and  $<0.075 \text{ cm}^{-1}$  bandwidth was produced. The MOPO output was then doubled in an angle-tuned KDP crystal and then finally frequency tripled in BBO crystal to produce vertically polarized 202 nm light. The tripled light was then focused with a 16 cm lens into the ionization chamber where the reactions of  $\text{N}_2^+$  ions with the target neutral molecule took place. The 202 nm laser beam was focused just in front of the nozzle. The ionization chamber was maintained at a pressure of  $1.0 \times 10^{-5}$  Torr (beam on). To reduce the dominance of the parent ion in the time-of-flight mass spectrum, we sometimes defocused the laser beam slightly. A typical molecular beam would, for example, contain  $\sim 1$ –5% pure  $\text{N}_2$  gas seeded in helium buffer gas along with a small amount ( $\sim 1$ –5%) of the reactant neutral species. Higher  $\text{N}_2$  concentrations were found to lead to broader mass spectra and evidence of secondary reactions. The conditions of the experiment were explored so that we could be assured that the measured BRs were not sensitive to laser delay, reactant concentration, pulsed valve delay, extraction voltages, and so on. In this way, we could be sure that the product BRs were exclusively from primary reactions. After  $\text{N}_2^+$  ionization and subsequent reaction with the target neutral molecule, the mixture was then allowed to expand supersonically without skimming the beam. There was no ion signal when the laser was off resonance, and there was no sign of

**Table 1.** Branching Ratios for the Formation of Various Product Ion Channels Observed upon the Reaction of  $\text{N}_2^+$  ( $\nu = 0$ ) with  $\text{CH}_4$ ,  $\text{C}_2\text{H}_2$ , and  $\text{C}_2\text{H}_4$ <sup>a</sup>

reaction	product ion	branching ratio
$\text{N}_2^+ + \text{CH}_4$	$\text{CH}_3^+$	$0.83 \pm 0.02$
	$\text{CH}_2^+$	$0.17 \pm 0.02$
$\text{N}_2^+ + \text{C}_2\text{H}_2$	$\text{C}_2\text{H}_2^+$	1
$\text{N}_2^+ + \text{C}_2\text{H}_4$	$\text{C}_2\text{H}_3^+$	$0.74 \pm 0.02$
	$\text{C}_2\text{H}_2^+$	$0.26 \pm 0.02$

<sup>a</sup> Branching ratios are an average of at least six independent measurements under similar conditions with  $\pm 2\sigma$  error.

other product ions (e.g.,  $\text{He}^+$ ,  $\text{C}^+$ ) suggesting plasma formation at the nozzle. The  $\text{N}_2$  REMPI spectrum was scanned in the same configuration, with the signal at  $m/z = 28$  or 16 (methane) recorded. These spectra were essentially identical, and they were fitted to yield a rotational temperature of  $\sim 45$  K. Although we did not measure the translational temperature directly, we believe it is unlikely to be significantly different from the measured rotational temperature.

The unskimmed molecular beam containing the newly born ions was allowed to flow downstream into the main chamber where ion extraction and detection were accomplished. The main chamber was maintained at  $5.0 \times 10^{-7}$  Torr. A constant negative bias of  $-50$  and  $-30$  V was independently applied to the repeller and the extractor plates, respectively. The plates were then separately pulsed for the extraction of the product ions, with the potentials optimized to give the best mass resolution. Both plates were externally triggered at 10 Hz with the same pulse width and delay time, which were occasionally adjusted and optimized to obtain the optimum mass resolution. After the extraction of the product ions, the ion cloud was accelerated toward a 120 mm diameter position-sensitive detector that consisted of a pair of chevron-type microchannel plates (MCPs) coupled to a fast P-47 phosphor screen. A CCD camera (SONY XC-ST50),  $768 \times 494$  pixels) was used to view the phosphor screen while a photomultiplier tube (PMT) was used to capture the integrated time-of-flight signal. In this particular case, the MCP was ungated and the PMT signal was sent to an oscilloscope for averaging, and the final data were transferred to the computer.

## RESULTS

**$\text{N}_2^+ + \text{CH}_4$  Reaction.** The time-of-flight mass spectrum for the reaction between  $\text{N}_2^+$  ( $\nu = 0$ ) ions with  $\text{CH}_4$  is presented in Figure 1. The spectrum was accumulated up to 1200 shots at 10 Hz with the accumulated intensity of the  $\text{CH}_3^+$  and  $\text{CH}_4^+$  product ions being measured and monitored for a period of 15–20 min to ensure that there was no change in the BRs. To eliminate the occurrence of secondary reactions, we kept  $\text{CH}_4$  concentrations low at  $\sim 1\%$ . The obtained mass spectra were then fitted using Gaussian functions, and the integrated area of the peaks was used to calculate the BRs presented in Table 1. The results summarized in Table 1 give an overall branching ratio of 0.83:0.17 for the formation of  $\text{CH}_3^+$  and  $\text{CH}_2^+$  product ions, respectively. Although it is energetically possible to form the  $\text{CH}_4^+$  ion, this nondissociative charge transfer was not observed in our experiment. Even at very low collision energies the integral



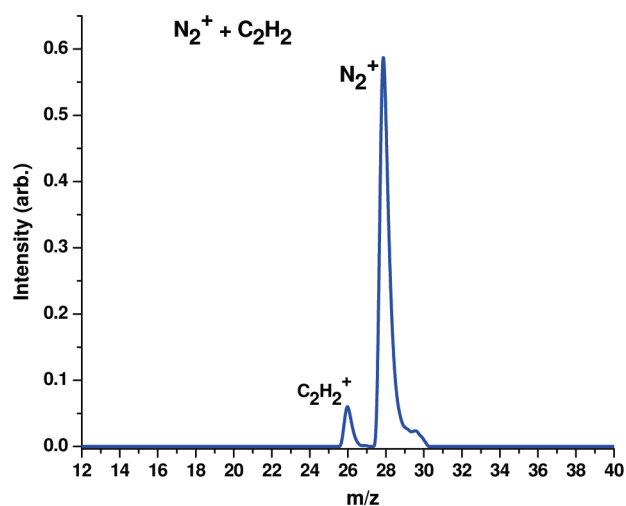


**Figure 2.** Time-of-flight spectrum of ionic products from the reaction of  $N_2^+$  ( $v = 0$ ) with acetylene.

cross section for this channel is  $<0.1 \text{ \AA}^2$ , as has already been reported by Nicolas et al.<sup>6</sup>

To gain more insight into the dynamics of the dissociative charge-transfer reaction of state-prepared  $N_2^+$  ion with  $CH_4$ , it is important to consider the dissociation pathways and the fragmentation pattern of  $CH_4^+$  ion, as reported by Stockbauer<sup>36</sup> and Bombach.<sup>37</sup> The ionization energy (IE) of  $CH_4$  is 12.61 eV, whereas the dissociation energy of  $CH_4^+$  leading to the formation of  $CH_3^+ + H$  channel is 1.64 eV.<sup>38</sup> The removal of an electron from  $CH_4$  molecule leads to the formation of nascent  $CH_4^+$  product ions in a triply degenerate  $^2T_2$  state.<sup>39</sup> Because of the Jahn–Teller effect,<sup>39</sup> the nascent  $CH_4^+$  cation then undergoes deformation to lower symmetry  $^2T_g$  structure. Between 13.8 and 16.4 eV, the  $CH_4^+$  ( $^2T_g$ ) ion exhibits a breakdown pattern<sup>40</sup> that leads to the formation of  $CH_4^+$  product ions only  $<14.3$  eV. Above 14.3 eV, the branching ratio to the  $CH_4^+$  product ion decreases because of the appearance of  $CH_3^+$  ion. The  $CH_4^+$  product ion disappears above 14.5 eV. The threshold for the formation of  $CH_2^+$  product ions is 15.2 eV, with its branching increasing with an increase in the internal energy. Taking into account the fact the IE of  $N_2$  is 15.58 eV,<sup>41</sup> this means that a significant amount of the 2.97 eV reaction exoergicity is deposited into  $CH_4^+$  ion in the form of internal energy. On the basis of this reported fragmentation pattern of  $CH_4^+$  ion below 16 eV, the absence of a  $CH_4^+$  ion peak in our mass spectrum is a confirmation that  $CH_4^+$  formation becomes insignificant as  $CH_3^+$  and  $CH_2^+$  ions are formed because of an increase in the internal energy of the parent  $CH_4^+$  product ion. The IE for  $Ar^+$ <sup>41</sup> is very close to that of  $N_2$ ; it is therefore worth comparing our present results to those of  $Ar^+ + CH_4$  reaction reported by Tsuji et al.<sup>42</sup> In the  $Ar^+ + CH_4$  reaction, Tsuji et al.<sup>42</sup> observed the formation of  $CH_3^+$  and  $CH_2^+$  product ions as the only primary channels, with an overall branching ratio of 0.85:0.15, respectively. This branching is very close to our present BR value for the formation of  $CH_3^+$  and  $CH_2^+$  product ions in the  $N_2^+ + CH_4$  reaction, which is in turn indicative of a similar charge-transfer reaction mechanism. In addition, our BR is also in reasonable agreement to the previous reported values at low temperature<sup>24</sup> and under room-temperature conditions.<sup>8</sup>

**$N_2^+ + C_2H_2$  Reaction.** The time-of-flight spectrum presented in Figure 2 shows the formation of  $C_2H_2^+$  ion as the only primary

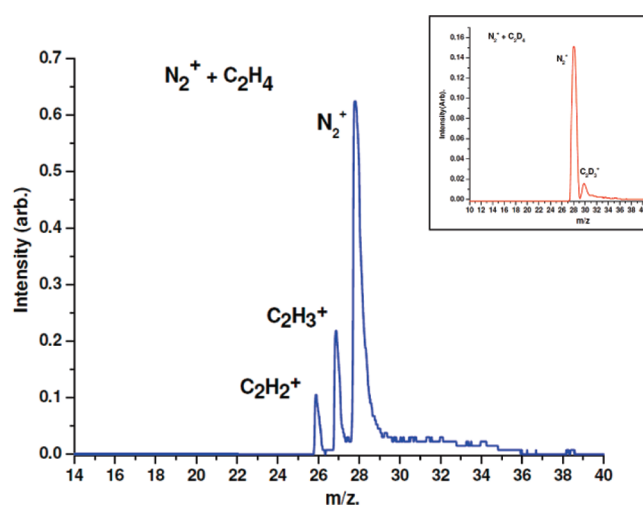


**Figure 3.** Time-of-flight spectrum of the product ion channels from the reaction of  $N_2^+$  ( $v = 0$ ) with  $C_2H_4$ . Inset shows the spectrum for reaction with  $C_2D_4$ , confirming the absence of  $C_2D_4^+$  product.

product channel in the  $N_2^+ + C_2H_2$  reaction. This is in agreement with the previous room-temperature measurements by Anicich et al.<sup>8</sup> using flowing afterglow-selected ion flow tube (FA-SIFT) technique. The single charge-transfer channel was observed to proceed with an overall rate constant of  $5.50 \times 10^{-10} \text{ cm}^3/\text{s}$ . The IE of  $C_2H_2$  is 11.4 eV.<sup>41</sup> This gives a value of 4.19 eV as the total amount of internal energy that can efficiently be transferred to the  $C_2H_2^+$  in a  $N_2^+ + C_2H_2$  collision and hence become available for bond-breaking in the parent  $C_2H_2^+$  cation. The appearance energy for the lowest energy dissociation channel in  $C_2H_2^+$  (i.e., the formation of  $C_2H^+$  ion) is 17.3 eV.<sup>41,43</sup> This value is higher than the IE of  $N_2^+$  and hence it is not energetically possible to induce C–H bond dissociation in  $C_2H_2^+$  through a dissociative charge-transfer reaction with  $N_2^+$ . Our present results are also in reasonable agreement with the almost isoenergetic  $Ar^+ + C_2H_2$  reaction,<sup>42</sup> where  $C_2H_2^+$  product ion was observed as the only product channel. The formation of  $C_2H_2^+$  ( $^2\Pi_u$ ) in the  $N_2^+ + C_2H_2$  reaction can simply be understood as an efficient charge-transfer reaction that occurs without an energy barrier in a direct long-range encounter.

**$N_2^+ + C_2H_4$  Reaction.** Figure 3 presents the associated time-of-flight spectrum for the  $N_2^+ + C_2H_4$  reaction. The main peaks observed in this experiment correspond to the formation of  $C_2H_3^+$  and  $C_2H_2^+$  product ions at a branching ratio of 0.74:0.26 (as shown in Table 1). At this point, it may be worthwhile to take into consideration the electronic states of  $C_2H_4^+$  ion that may be involved in the charge-transfer reaction below 15.58 eV, the limit for our recombination energy. The four main  $C_2H_4^+$  precursor states that may be involved are  $X^2B_{2u}$ ,  $A^2B_{2g}$ ,  $B^2A_{2g}$ , and  $C^2B_{3u}$ .<sup>44,45</sup> The removal of an electron from any of these states results in C–H bond(s) rupture. As mentioned by Tsuji et al.<sup>42</sup> in the  $Ar^+ + C_2H_4$  ion–molecule reaction, the CT reaction in  $C_2H_4$  predominantly leads to an efficient population of a predissociative  $C_2H_4^+$  state that lies at about the 15.3 eV energy range. From the  $C_2H_4$  breakdown diagram,<sup>37</sup>  $C_2H_4^+$  ion can be formed only below 13.3 eV. The production of the parent ion starts to decrease above 13.0 eV because of the appearance of  $C_2H_3^+$  and  $C_2H_2^+$  product ions. In the  $Ar^+ + C_2H_4$  reaction, for example, the formation of  $C_2H_4^+$  nondissociative CT channel

was negligible with a reported BR of 0.04 as compared with the  $C_2H_3^+ : C_2H_2^+$  BR of 0.76:0.20. This reported BR for the formation of  $C_2H_3^+$  and  $C_2H_2^+$  product ions was found to increase with an increase in the internal energy of the parent  $C_2H_4^+$  ion. The present 0.74:0.26 BR for the formation of  $C_2H_3^+$  and  $C_2H_2^+$  product ions, respectively, is not very different from the one observed for the  $Ar^+ + C_2H_4$  reaction in Tsuji et al.'s work.<sup>42</sup> We do not anticipate that the  $C_2H_4^+$  product channel would be formed because it is expected to undergo a rapid decomposition to  $C_2H_3^+$  and  $C_2H_2^+$  product ions. Owing to interference from  $N_2^+$  at  $m/z = 28$ , we could not exclude the possibility of a  $C_2H_4^+$  product in that reaction. However, by using  $C_2D_4$  as a reactant, as shown in the inset in Figure 3, we have confirmed the absence of a simple charge transfer channel giving ethylene cation. To gain deeper insight into the dynamics of this  $N_2^+$  ion–molecule reaction, these results will be further discussed in the following section by invoking the photoionization and the state-specific photodissociation dynamics results of  $C_2H_4^+$  cation as reported in previous studies.

## DISCUSSION

**$N_2^+ + CH_4$  Reaction: Dissociative Charge Transfer and the Branching Ratios.** Despite the uncertainty in the BR measurements by different techniques and workers, it is generally accepted that the mechanism accompanying this reaction is a simple capture process, followed by dissociative charge-transfer. It is instructive to discuss our results in relation to the previous results of  $Ar^+ + CH_4$  reaction by Tsuji et al.<sup>42</sup> In the  $Ar^+ + CH_4$  reaction, the dissociative charge transfer leading to the formation of  $CH_3^+$  and  $CH_2^+$  product ions is thought to involve a nonadiabatic transition between two nonresonant charge states,  $Ar^+ + CH_4$  and  $CH_4^+ + Ar$ . As indicated by the magnitude of the total cross-section, there is a large nonadiabatic coupling between these two charge transfer states. Upon reaching the first relevant crossing that has a high probability,  $Ar^+$  and  $CH_4$  charge transfer occurs with unit probability resulting in an immediate dissociation of the nascent  $CH_4^+$  ion. Although a detailed potential energy surface for the reaction  $N_2^+ + CH_4$  is not currently available, it is likely that the dissociative charge transfer reaction proceeds via a nonadiabatic coupling just as in the  $Ar^+ + CH_4$  case. In a previous study, Nicolas et al.<sup>10</sup> proposed that the formation of  $CH_2^+$  and  $CH_3^+$  ions proceeds via a separated sequential process. In this case, an impulsive single-electron transfer is later accompanied by  $CH_4^+$  ion dissociation.

Using a flow jet reactor, Randeniya and Smith<sup>24</sup> obtained a  $CH_3^+ : CH_2^+$  branching ratio of 0.80:0.20 at 30 K, a value that is very close to our present  $40 \pm 5$  K value of 0.83:0.17. The room-temperature branching ratio of 0.88:0.12 reported by Anicich et al.<sup>8</sup> differs by  $\sim 7\%$  with our value. It is critical to mention that the  $CH_3^+ : CH_2^+$  branching ratio does not depend significantly on the collision energy, an indication that the kinetic energy is not efficiently converted to internal energy of the  $CH_4^+$  ion. As previously noted in the Nicholas et al. study, this behavior is also a confirmation of the strong coupling between the two aforementioned charge states ( $N_2^+ + CH_4$  and  $CH_4^+ + N_2$ ).

**Charge Transfer in  $N_2^+ + C_2H_2$  Reaction.** High-resolution He I photoelectron spectroscopy shows that the adiabatic IEs corresponding to  $X^2\Pi_u$ ,  $A^2\Sigma_g^+$ , and  $B^2\Sigma_u^+$  states of  $C_2H_2^+$  ion are 11.403, 16.297, and 18.391 eV,<sup>45</sup> respectively. There also exist regions of autoionizing Rydberg series that converge to vibrationally excited levels of the electronic ground state at

regions 2 eV above the ground state. It is plausible that these autoionizing Rydberg states act as the precursors to the non-dissociative charge transfer reaction that lead to the sole formation of  $C_2H_2^+$  product ion. Because the threshold for the appearance of the lowest H-loss dissociation channel,  $C_2H^+ + H$ , is above the recombination energy of  $N_2^+$  ion (15.58 eV), the only accessible electronic state in a  $C_2H_2$  collision encounter with  $N_2^+$  is the  $X^2\Pi_u$  ground state. Because no chemical bond is broken in the  $C_2H_2^+$  ion, the appearance of a single peak as displayed in Figure 2 is as a result of a CT process that occurs over comparatively long distances in an electron transfer that is accompanied by no appreciable momentum change. Considering the  $N_2^+$  ion recombination energy of 15.58 eV and the strong C–H bond in  $C_2H_2^+$  cation, the nondissociative CT channel leading to the formation of  $C_2H_2^+$  product ion is expected to be the only primary process. This is consistent with our observed unity measurement of the branching for this reaction.

**$N_2^+ + C_2H_4$  Reaction: Dissociative Charge Transfer and the Branching Ratio.** Our time-of-flight mass spectrum shown in Figure 3 represents the first unambiguous experimental study identifying  $C_2H_3^+$  and  $C_2H_2^+$  as the major primary product channels in the  $N_2^+ + C_2H_4$  charge transfer reaction. The branching ratio for the formation of  $C_2H_3^+ : C_2H_2^+$  product ions as summarized in Table 1 is 0.74:0.26, respectively. In their most recent work, Anicich et al.<sup>8</sup> performed careful modeling of the  $N_2^+ + C_2H_4$  reaction and followed the reactions over a significant flow range. Whereas the  $HCN^+$  and  $HCNH^+$  channels previously reported by Anicich et al. were omitted in the model, the nondissociative charge-transfer channel was also not identified. A branching ratio of 0.64:0.36 for the  $C_2H_3^+ : C_2H_2^+$  product channels was obtained from the model. Our BR measurement differs by  $\sim 9\%$  from that inferred from the model. To get more insight into the  $N_2^+ + C_2H_4$  dissociative charge transfer reaction that leads to the observed branching ratio, it is beneficial to consider the excited states of the  $C_2H_4^+$  cation that may be involved. As previously mentioned, below 16 eV, the four  $C_2H_4^+$  accessible states are:  $X^2B_{3u}$ ,  $A^2B_{3g}$ ,  $B^2A_g$ , and  $C^2B_{2u}$  states at 10.51, 12.45, 14.45, and 15.87 eV, respectively.<sup>46</sup> The appearance energies for the formation of  $C_2H_3^+$  and  $C_2H_2^+$  ions are 13.3 and 13.0 eV, respectively.<sup>46</sup> This clearly shows that at a total  $N_2^+$  recombination energy of 15.58 eV the  $C_2H_3^+$  and  $C_2H_2^+$  ions have thresholds that are associated with the  $X^2B_{3u}$  and  $A^2B_{3g}$  as the possible precursor electronic states. We note here that to have a clear picture of the dynamics involved in the CT reaction of  $N_2^+ + C_2H_4$ , one cannot overlook the underlying photodissociation dynamics of the  $C_2H_4^+$  cation and the associated branching as exemplified in a number of previous studies. Indeed, a detailed state-selected ion imaging study on  $C_2H_4^+$  cation dissociation by Kim et al.<sup>30</sup> has established that the  $C_2H_4^+$  cation undergoes fragmentation that leads to H loss and  $H_2$  elimination as the main primary processes. Consistent with the previous single-photon ionization mass spectrometry and threshold–photoelectron–photoion coincidence (TPEPICO) studies,<sup>36</sup> Kim et al.<sup>30</sup> found the H-elimination channel to be much more favorable than the  $H_2$ -loss channel. It is interesting to note that just as in these photochemistry experiments the most preferred dissociative CT channel in our present study is the H-loss channel leading to the formation of  $C_2H_3^+$  production. Although  $Ar^+$  is more energetic than  $N_2^+$  ion (15.76 recombination energy versus 15.58 eV), its reactions with  $C_2H_4$  provide an additional platform for obtaining a qualitative picture of the charge-transfer mechanism for the reactions of  $N_2^+$  with  $C_2H_4$ . The  $Ar^+ + C_2H_4$  study<sup>42</sup> reported a branching of 0.76:0.20:0.04 for  $C_2H_2^+ : C_2H_3^+ : C_2H_4^+$  with a conclusion that the  $C_2H_2^+$  and  $C_2H_3^+$  ions are produced through a near-resonant charge transfer mechanism without

significant momentum transfer. Consequently, two charge transfer mechanisms in the  $\text{Ar}^+ + \text{C}_2\text{H}_4$  reaction are inferred; one is the dominant near-resonant dissociative charge transfer leading to the formation of  $\text{C}_2\text{H}_3^+$  and  $\text{C}_2\text{H}_2^+$  ions, whereas the other is the minor nonresonant nondissociative charge transfer leading to the formation of  $\text{C}_2\text{H}_4^+$  parent ions. In the  $\text{N}_2^+ + \text{C}_2\text{H}_4$  reaction, we propose that just as in the case of  $\text{N}_2^+ + \text{CH}_4$  reaction, the collision encounter between  $\text{N}_2^+$  ions and the  $\text{C}_2\text{H}_4$  molecule lead to an efficient dissociative charge transfer involving a nonadiabatic transition between two nonresonant charge states of  $\text{N}_2^+ + \text{C}_2\text{H}_4$  and  $\text{C}_2\text{H}_4^+ + \text{N}_2$ . Detailed theoretical studies on the potential energy surface for the reaction  $\text{N}_2^+ + \text{C}_2\text{H}_4$  would be required to validate our proposed mechanism, but owing to the similarities between the recombination energies of  $\text{Ar}^+$  and  $\text{N}_2^+$  ions, this interpretation appears to be quite plausible. Our qualitative arguments can be further supported by the fact that we do not observe the parent  $\text{C}_2\text{H}_4^+$  ion.

## CONCLUSIONS AND IMPLICATIONS FOR TITAN'S ATMOSPHERE

The BRs of the reactions of state-prepared  $\text{N}_2^+$  ion with  $\text{CH}_4$ ,  $\text{C}_2\text{H}_2$ , and  $\text{C}_2\text{H}_4$ , the main minor hydrocarbon constituents of Titan's upper atmosphere, have been measured at a characteristic temperature of  $45 \pm 5$  K. The dominant reaction channels in the  $\text{N}_2^+ + \text{CH}_4$  and  $\text{N}_2^+ + \text{C}_2\text{H}_2$  reactions are the nonresonant dissociative CT, whereas for the  $\text{N}_2^+ + \text{C}_2\text{H}_4$  reaction, the nondissociative CT channel leading to the sole formation of  $\text{C}_2\text{H}_2^+$  product ion is the only reaction channel. In the  $\text{N}_2^+ + \text{CH}_4$  reaction, a branching ratio of 0.83:0.17 is obtained for the formation of  $\text{CH}_3^+$  and  $\text{CH}_2^+$  product ions, respectively. The absence of a nondissociative  $\text{CH}_4^+$  charge transfer channel suggest that the dominant process in this reaction is a near-resonant CT process that is accompanied by simple C–H bond rupture of the nascent  $\text{CH}_4^+$  ion. Results for the  $\text{N}_2^+ + \text{C}_2\text{H}_4$  reaction indicate that  $\text{C}_2\text{H}_3^+$  and  $\text{C}_2\text{H}_2^+$  product ions are formed at a branching ratio of 0.74:0.26, respectively. The process associated with this observed branching is a simple capture process, followed by a nonresonant dissociative CT. This present study represents the most reliable experimental data on the primary branching ratios of the main product channels in low-temperature reaction of  $\text{N}_2^+$  with  $\text{CH}_4$ ,  $\text{C}_2\text{H}_2$ , and  $\text{C}_2\text{H}_4$ . This primary branching also gives a direct insight into the dynamics associated with these ion–molecule reactions in Titan's rich ionospheric chemistry. The reported branching ratio measurements illustrate a new, promising modification of a VMIMS apparatus that allows for direct determination of branching ratios of state specific ion–molecule reactions at low temperatures prevalent in Titan's upper atmosphere.

## AUTHOR INFORMATION

### Corresponding Author

\*E-mail: asuits@chem.wayne.edu.

## ACKNOWLEDGMENT

This work was supported by the NSF under award number CHE-0627854. We thank Nuradhika Herath and Stephanie Everhart or their assistance with the experiment.

## REFERENCES

- (1) Ng, C.-Y. *J. Phys. Chem. A* **2002**, *106*, 5953.
- (2) Mahan, B. H. *Acc. Chem. Res.* **1968**, *1*, 217.
- (3) Farrar, J. M.; Lee, Y. T. *Annu. Rev. Phys. Chem.* **1974**, *25*, 357.
- (4) Boyle, J. M.; Uselman, B. W.; Liu, J.; Anderson, S. L. *J. Chem. Phys.* **2008**, *128*, 114304.
- (5) Dressler, R. A.; Chiu, Y.; Levandier, D. J.; Tang, X. N.; Hou, Y.; Chang, C.; Houchins, C.; Xu, H.; Ng, C.-Y. *J. Chem. Phys.* **2006**, *125*, 132306.
- (6) Nicolas, C.; Torrents, R.; Gerlich, D. *J. Chem. Phys.* **2003**, *118*, 2723.
- (7) Qian, X.-M.; Zhang, T.; Chang, C.; Wang, P.; Ng, C. Y.; Chiu, Y.-H.; Levandier, D. J.; Miller, J. S.; Dressler, R. A.; Baer, T.; Peterka, D. S. *Rev. Sci. Instrum.* **2003**, *74*, 4096.
- (8) Anicich, V. G.; Wilson, P.; McEwan, M. J. *J. Am. Soc. Mass Spectrom.* **2004**, *15*, 1148.
- (9) Anicich, V. G.; McEwan, M. J. *Planet. Space Sci.* **1997**, *45*, 897.
- (10) Balucani, N.; Asvany, O.; Osamura, Y.; Huang, L. C. L.; Lee, Y. T.; Kaiser, R. I. *Planet. Space Sci.* **2000**, *48*, 447.
- (11) Kaiser, R. I.; Ochsenfeld, C.; Head-Gordon, M.; Lee, Y. T.; Suits, A. G. *Science* **1996**, *274*, 1508.
- (12) Sims, I. R.; Smith, I. W. M. *Chem. Phys. Lett.* **1988**, *151*, 481.
- (13) Smith, I. W. M. *Angew. Chem., Int. Ed.* **2006**, *45*, 2842.
- (14) Imanaka, H.; Smith, M. A. *Proc. Natl. Acad. Sci. U.S.A.* **2010**, *107*, 12423.
- (15) Thissen, R.; Vuitton, V.; Lavvas, P.; Lemaire, J.; Dehon, C.; Dutuit, O.; Smith, M. A.; Turchini, S.; Catone, D.; Yelle, R. V.; Pernot, P.; Somogyi, A.; Coreno, M. *J. Phys. Chem. A* **2009**, *113*, 11211.
- (16) Ascenzi, D.; Aysina, J.; Tosi, P.; Maranzana, A.; Tonachini, G. *J. Chem. Phys.* **2010**, *133*, 184308.
- (17) Wilson, E. H.; Atreya, S. K. *Planet. Space Sci.* **2003**, *51*, 1017.
- (18) Yelle, R. V.; Borggren, N.; de la Haye, V.; Kasprzak, W. T.; Niemann, H. B.; Müller-Wodarg, I.; Waite, J. J. H. *Icarus* **2006**, *182*, 567.
- (19) McEwan, M. J.; Anicich, V. G. *Mass Spectrom. Rev.* **2007**, *26*, 281.
- (20) McEwan, M. J.; Scott, G. B. I.; Anicich, V. G. *Int. J. Mass Spectrom.* **1998**, *172*, 209.
- (21) Carrasco, N.; Alcaraz, C.; Dutuit, O.; Plessis, S.; Thissen, R.; Vuitton, V.; Yelle, R.; Pernot, P. *Planet. Space Sci.* **2008**, *56*, 1644.
- (22) Carrasco, N.; Dutuit, O.; Thissen, R.; Banaszkiewicz, M.; Pernot, P. *Planet. Space Sci.* **2007**, *55*, 141.
- (23) Suits, A. G. *J. Phys. Chem. A* **2009**, *113*, 11097.
- (24) Randeniya, L. K.; Smith, M. A. *J. Chem. Phys.* **1991**, *94*, 351.
- (25) Imanaka, H.; Smith, M. A. *J. Phys. Chem. A* **2009**, *113*, 11187.
- (26) Pollard, J.; Lichtin, D.; Cohen, R. *Chem. Phys. Lett.* **1988**, *152*, 171.
- (27) Glenewinkel-Meyer, T.; Gerlich, D. *Israel J. of Chem* **1997**, *37*, 343.
- (28) Belikov, A. E.; Mullen, C.; Smith, M. A. *J. Chem. Phys.* **2001**, *114*, 6625.
- (29) Leskiw, B. D.; Kim, M. H.; Hall, G. E.; Suits, A. G. *Rev. Sci. Instrum.* **2005**, *76*.
- (30) Kim, M. H.; Leskiw, B. D.; Suits, A. G. *J. Phys. Chem. A* **2005**, *109*, 7839.
- (31) Gichuhi, W. K.; Suits, A. G., in preparation.
- (32) Lykke, K. R.; Kay, B. D. *J. Chem. Phys.* **1991**, *95*, 2252.
- (33) Kim, H.-T.; Anderson, S. L. *J. Chem. Phys.* **2001**, *114*, 3018.
- (34) Conaway, W. E.; Morrison, R. J. S.; Zare, R. N. *Chem. Phys. Lett.* **1985**, *113*, 429.
- (35) Rijs, A. M.; Backus, E. H. G.; de Lange, C.; Janssen, M. H. M.; Wang, K.; V., M. J. *J. Chem. Phys.* **2001**, *114*, 9413.
- (36) Stockbauer, R. *J. Chem. Phys.* **1973**, *58*, 3800.
- (37) Bombach, R.; Dannacher, J.; Stadelmann, J.-P. *Int. J. Mass Spectrom. Ion Processes* **1984**, *58*, 217.
- (38) Berkowitz, J.; Greene, J. P.; Cho, H.; Ruscic, B. *J. Chem. Phys.* **1987**, *86*, 674.
- (39) Frey, R. F.; Davidson, E. R. *J. Chem. Phys.* **1988**, *88*, 1775.
- (40) Milhaud, J. *Int. J. Mass Spectrom. Ion Processes* **1975**, *16*, 327.
- (41) NIST Webbook. <http://webbook.nist.gov/chemistry/>.
- (42) Tsuji, M.; Kouno, H.; Matsumura, K.-i.; Funatsu, T.; Nishimura, Y.; Obase, H.; Kugishima, H.; Yoshida, K. *J. Chem. Phys.* **1993**, *98*, 2011.

- (43) Mackie, R. A.; Scully, S. W. J.; Sands, A. M.; Browning, R.; Dunn, K. F.; Latimer, C. J. *Int. J. Mass Spectrom.* **2003**, 223–224, 67.
- (44) Turner, D. W.; Baker, A. D; Brundle, C. R. *Molecular Photoelectron Spectroscopy*; Wiley-Interscience: New York, 1970.
- (45) Kimura, K.; Katsumata, K., Achiba, Y.; Yamazaki, T.; Iwata, S. *Handbook of He Photoelectron Spectra of Fundamental Organic Molecules. Ionization Energies, Ab Initio Assignments, and Valence Electronic Structure for 200 Molecules*; Tokyo and Halstead Press: New York, 1981.
- (46) Pollard, J. E.; Trevor, D. J.; Reutt, J. E.; Lee, Y. T.; Shirley, D. A. *J. Chem. Phys.* **1984**, 81, 5302.